Research Square

Preprints are preliminary reports that have not undergone peer review.
They should not be considered conclusive, used to inform clinical practice,
or referenced by the media as validated information.

The polyol pathway and nuclear ketohexokinase A signaling drive hyperglycemia-induced metastasis of gastric cancer

Ye-Lim Kang
Seoul National University College of Medicine
Jiyoung Kim
Seoul National University College of Medicine
Yi-Sook Kim
Seoul National University College of Medicine
Jong-Wan Park (parkjw@snu.ac.kr)
Seoul National University College of Medicine

Research Article

Keywords: Diabetes mellitus, gastric cancer metastasis, fructose, AKR1B1, KHK-A

Posted Date: December 7th, 2022

DOI: https://doi.org/10.21203/rs.3.rs-2345829/v1

License: This work is licensed under a Creative Commons Attribution 4.0 International License.
Read Full License

Abstract

Background: Diabetes is significantly associated with increased cancer risk, with several studies reporting hyperglycemia as a primary oncogenic stimulant. Glucose metabolism is linked to numerous metabolic pathways, making it difficult to specify the mechanisms underlying hyperglycemia-induced cancer progression. Here, we focused on the polyol pathway, which is dramatically activated under hyperglycemia and causes diabetic complications. We tested the possibility that polyol pathway-derived fructose facilitates hyperglycemia-induced gastric cancer metastasis.

Methods: We performed bioinformatics analysis of gastric cancer datasets and immunohistochemical analyses of gastric cancer specimens, followed by transcriptomic and proteomic analyses to evaluate phenotypic changes in gastric cancer cells. We used two xenograft models to evaluate gastric cancer metastasis in patients with diabetes.

Results: We observed a clinical association between the polyol pathway and gastric cancer progression. In gastric cancer cell lines, hyperglycemia enhanced cell migration and invasion, cytoskeletal rearrangement, and epithelial-mesenchymal transition (EMT). The hyperglycemia-induced acquisition of metastatic potential was mediated by increased fructose derived from the polyol pathway, which stimulated the nuclear ketohexokinase-A (KHK-A) signaling pathway, thereby inducing EMT by repressing the *CDH1* gene. In two different xenograft models of cancer metastasis, gastric cancers overexpressing AKR1B1, which catalyzes the rate-limiting step in the polyol pathway, were found to be highly metastatic in diabetic mice.

Conclusions: Hyperglycemia induces fructose formation through the polyol pathway, which in turn stimulates the KHK-A signaling pathway, driving gastric cancer metastasis by inducing EMT. Thus, the polyol and KHK-A signaling pathways could be potential therapeutic targets for lowering the metastatic risk in gastric cancer patients with diabetes.

Background

The incidence and prevalence of diabetes and cancer have been increasing worldwide. As of 2017, more than 450 million people have been diagnosed with diabetes[1], and the incidence of cancer, excluding skin cancer, was approximately 20 million new cases per year[2]. Approximately 60% of newly diagnosed cancer patients are over the age of 65[3], and approximately 25% of people over the age of 65 also have diabetes[4]. Thus, 8–18% of cancer patients are accompanied by diabetes in the overall population[5], and diabetes is a frequent comorbidity of cancer patients in the elderly group over 65 years of age[6, 7]. Recently, several clinical cohort studies have demonstrated that diabetes is a major risk factor for several cancers[8–10]. Moreover, studies have reported that diabetes is associated with the incidence, mortality, and progression of various cancers[6, 11–13]. Experimental studies[14–16] have revealed that hyperglycemia *per se*, rather than the common risk factors between diabetes and cancer, worsens cancer. Hyperglycemia renders cancer cells more aggressive by exerting metabolic and oxidative stresses[16–18].

Glucose metabolism involves multiple intertwined metabolic pathways, dynamically generating numerous glucose metabolites, which affect cancer cell fate and behavior. For example, in the polyol pathway, aldo-keto reductase-1-member-1 (AKR1B1) reduces glucose to sorbitol, and sorbitol dehydrogenase (SORD) converts sorbitol to fructose. Normally, only ~ 3% of glucose is metabolized through the polyol pathway, but under hyperglycemia, over 30% of the glucose enters the pathway due to saturation of hexokinase action [19, 20]. The polyol pathway is involved in the development of diabetic complications[21]. Under hyperglycemia, the polyol pathway depletes NADPH and also generates excess NADH, resulting in a redox imbalance. Moreover, fructose generates Advanced Glycation End products (AGEs), facilitating oxidative stress. In addition, increased osmotic pressure due to sorbitol accumulation aggravates diabetic complications, such as neuropathy, nephropathy, and retinopathy[21]. Several recent reports have demonstrated that the polyol pathway is involved in cancer progression and metastasis[22–24]. AKR1B1 has been reported to be overexpressed in several cancer types[25, 26]. AKR1B1 inhibition suppresses cancer growth[24] and its activation induces epithelial-mesenchymal transition (EMT) to facilitate cancer migration and invasion[22, 23]. Nevertheless, little is known about the molecular mechanisms by which the polyol pathway promotes cancer progression.

Here, we investigated the role of the polyol pathway in the hyperglycemia-induced metastasis of gastric cancer. Hyperglycemia facilitated migration and invasion of gastric cancer cells depending on the polyol pathway. In two xenograft models of gastric cancer, AKR1B1 overexpression increased metastasis in diabetic mice. Mechanistically, the polyol pathway-derived fructose activated the KHK-A-YWHAH-SLUG pathway to induce EMT by repressing the *CDH1* gene. In conclusion, the polyol pathway promotes diabetes-induced gastric cancer metastasis by activating the KHK-A signaling pathway.

Methods

Cell lines and Materials

Human gastric cancer cell lines AGS, MKN-1, MKN-28, and MKN-45 were obtained from American Type Culture Collection (ATCC; Manassas, VA); SNU-216, SNU-484, SNU-601, and SNU-638 from Korean Cell Line Bank (Seoul, South Korea). Cells were cultured with 10% heat-inactivated fetal bovine serum in RPMI or in DMEM at 37°C under 5% CO_2. For high glucose (HG) conditions, cells were incubated in the media supplemented with 50 mM glucose. Culture media, serum, Epalrestat, and Streptozocin were purchased from Sigma-Aldrich (St. Louis, MO). Antibodies used in this work are listed in Supplementary Table 1.

Preparation of plasmids, siRNAs and transfection

The cDNAs for human *AKR1B1*, *SORD*, *KHK-A*, and *YWHAH* were cloned by reverse transcription and PCR using Pfu DNA polymerase, and inserted into pcDNA-Myc, pcDNA-His, or pcDNA-FLAG vectors. For transient expression and knock-down, cells at ~ 70% were transfected using Jet-Prime reagent (Polyplus, Illkirch, France) and Lipofectamine RNAiMAX reagent (Invitrogen), respectively. Nucleotide sequences of siRNAs are summarized in Supplementary Table 2.

Gastric cancer xenografts

All animal experiments were carried out with the proposed protocol approved by the Institutional Animal Care and Use Committee (approval No. SNU-190702-3-3). MKN-28 and SNU-638 gastric cancer cells were transfected with the luciferase-IRES-GFP plasmid or the luciferase-IRES-AKR1B1 plasmid and selected using G418 (Millipore, Burlington, MA). Male 8-week-old Balb/cSlc-nu/nu mice were *i.p.* injected with streptozotocin (100 mg/kg) five times for 3 weeks. On the 10th week after the first streptozotocin injection, Transfected MKN-28 and SNU-638 were implanted in the spleen and subcutaneously injected into the left flank of mice, respectively. After 4 weeks (MKN-28) or 15 weeks (SNU-638), mice were *i.p.* injected with VivoGlo luciferin (Promega). Tumor were monitored using Xenogen IVIS100 with LivingImage 2.50.1 (Xenogen, Alameda, CA).

Cell migration and invasion assays

For migration analysis, cells in serum-free RPMI were seeded onto the upper chamber with an 8.0 μm pore filter (Corning Life Science, Acton, MA), and the lower chamber was filled with 10% serum. For invasion analysis, the Matrigel-coated filter was used. After 18 hr-inbubation, cells on the lower surface of the filter were fixed, stained with H&E, photographed, and counted using the ImageJ software (NIH, Bethesda, MD).

Quantitative RT-PCR

Total RNAs were extracted using TRIZOL reagent (Invitrogen), and reverse-transcribed using M-MLV Reverse Transcriptase (Enzynomics; Daejeon, Korea) at 42°C for 60 min. Real-time PCR was performed in the qPCR Mastermix (Enzynomics) using CFX Connect Real-Time Cycler (BIORAD, Hercules, CA). The mRNA levels were calculated in reference to the GAPDH level. All reactions were performed in triplicates. The nucleotide sequences of PCR primers are summarized in Supplementary Table 3.

Chromatin immunoprecipitation

Cells were fixed with 1% formaldehyde, lysed with 0.5% NP-40, and centrifuged at 800×g to collect nuclei. The pellet was lysed with 1% SDS, sonicated, incubated with IgG, anti-SLUG or anti-SNAIL antibody, and the immune complexes were pulled down using protein A/G beads (Santa Cruz Biotechnology). DNAs in the precipitates were extracted by phenol-chloroform-isoamyl alcohol (25:24:1), precipitated with ethanol, resolved in water, and subjected to PCR. Results were represented as the percentages of the input signal.

Immunoblotting and immunoprecipitation

Proteins were subjected to SDS-PAGE and transferred to Immobilon-P (Millipore). The membranes were incubated with primary and HRP-conjugated secondary antibodies in 5% skim milk, and visualized using the ECL plus kit (Amersham Biosciences; Piscataway, NJ). To analyze protein interactions, cell lysates were incubated with anti-MYC or anti-FLAG beads. The bound proteins were eluted using SDS or MYC/FLAG-tag peptides, and loaded on SDS-PAGE. All experiments were performed three or more times.

Immunohistochemistry and Immunofluorescence

For immunohistochemistry, tissue slides were deparaffinized, rehydrated, and heated to retrieve antigen. The slides were sequentially incubated with 3% H_2O_2, 2% horse serum, primary antibodies, and biotinylated secondary antibodies. The slides were treated with the DAB detection kit (Dako), counterstained with hematoxylin, and photographed at four high-power fields for each slide. Protein expression was analyzed using histoscore (the staining intensity (0–3) x the percentage of positive cells). Human gastric cancer tissue arrays were obtained from SuperBioChips (Seoul, Korea). Clinical information on patients is summarized in Supplementary Table 4. For immunofluorescence, cells on a cover slide were fixed with 4% paraformaldehyde, permeabilized with 0.1% Triton-X-100 and 0.05% Tween-20, and sequentially incubated with primary antibodies and Alexa Fluor 488-conjugated secondary antibodies (Invitrogen). F-actin was stained with Alexa Fluor 488 phalloidin (Abcam). After incubated with DAPI (Sigma-Aldrich), the slides were mounted in Faramount aqueous mounting medium (Dako). Fluorescence images were observed under a confocal microscope.

Mass analysis to quantify intracellular fructose

Cell pellets were vortexed with an ice-cold extraction solvent (Acetonitril:Methanil:Water = 4:4:2, v/v/v) for 1 min and snap-frozen for 1 min, and centrifuged at 10,000x*g* for 15 min. After subjected to SpeedVac, the dried samples were dissolved in 50 µL of water, which were subjected to LC-MS analysis. Sample separation was performed on a Hypersil Gold Amino column (150 X 2.1 mm, 1.9 µm, Thermo scientific) using an Ultimate 3000 (Dionex; Idstein, Germany) with isocratic elution. The UPLC system was coupled to a Q-Exactive Plus (Thermo Scientific) equipped with a heated electrospray ionization (HESI) source. The MS were operated in negative ion mode and the scan range was from m/z 50 to 500 in the targeted-sim mode. The standard fructose was obtained from Sigma-Aldrich.

Bioinformatics analysis

Public data for mRNA levels in gastric cancer patients were obtained from the GSE54129 (n = 132), GSE84437 (n = 433), GSE2685 (n = 30), and The Cancer Genome Atlas (TCGA) datasets. For survival analysis, 25 different types of cancer datasets from TCGA were used and samples of each type of cancer were categorized into AKR1B1 low expression group and AKR1B1 high expression group by median value. Kaplan-Meier overall survival graphs were analyzed using the GraphPad Prism software.

Statistical analysis

All data were analyzed using the Microsoft Excel 2013 or the GraphPad Prism 5.0. Results were expressed as the means and standard deviation (SD) from three or more samples. The unpaired, two-sided Student's *t*-test or Mann–Whitney U-test was used for statistical analyses. Spearman correlation analysis was used to measure the correlation coefficient between AKR1B1 and CDH1 expression in GSE2685 dataset. All statistical significances were considered when P values were less than 0.05.

Results

The polyol pathway is associated with gastric cancer progression

To examine if the polyol pathway is involved in gastric cancer progression, we focused on AKR1B1 because it determines the activity of the polyol pathway as the rate-limiting step. AKR1B1 levels were increased in gastric cancer tissue compared to normal stomach tissue (Fig. 1A). The Cancer Genome Atlas (TCGA) revealed that AKR1B1 expression is higher in metastatic or in lymph node metastatic stomach cancers (Fig. 1B and 1C). In gastric cancer patients, overall survival was lower in the AKR1B1-high group than in the AKR1B1-low group (Fig. 1D). In other types of cancers, however, AKR1B1 expression was not associated with clinical outcomes (Supplementary Fig. 1). Two enzymes AKR1B1 and SORD in the polyol pathway were analyzed in human gastric cancer tissues (Fig. 1E). When the specimens were divided into the low (I and II) and high (III and IV) stage groups, AKR1B1 and SORD levels were elevated in the high stage group (Fig. 1F). A chi-square analysis revealed that gastric cancers with elevated expression of both AKR1B1 and SORD are more aggressive (Fig. 1G). Moreover, the protein levels were higher in the metastatic group (Fig. 1H), and the high expression of both proteins was associated with metastasis (Fig. 1I). Collectively, these clinical data suggest that the polyol pathway is associated with the gastric cancer progression.

High glucose enhances the metastatic potential in gastric cancer

Given the polyol pathway (Fig. 2A), we hypothesized that high glucose facilitates cancer metastasis by increasing fructose via the polyol pathway. We checked the levels of AKR1B1 and SORD in gastric cancer cell lines (Supplementary Fig. 2A) and selected AGS and MKN-45, which express either AKR1B1 or SORD, for subsequent experiments. Both high glucose and fructose facilitated cell migration and invasion (Fig. 2B and Supplementary Fig. 2B, C). In AGS cells, high glucose and fructose induced F-actin rearrangement with filopodia-like cellular extensions (Fig. 2C), indicating that the cells undergo EMT. Of EMT markers, CDH1 (alternatively named E-cadherin) was markedly downregulated under high glucose and fructose conditions (Fig. 2D and Supplementary Fig. 2D). Thus, high glucose and fructose likely enhance the metastatic potential in gastric cancer cells by inducing EMT.

Under high glucose conditions, the polyol pathway-derived fructose mediates EMT and cell migration

The efficacies of AKR1B1- and SORD-targeting siRNAs were verified in AGS cells (Supplementary Fig. 3A). Under euglycemic conditions, cell migration was attenuated by silencing AKR1B1 or SORD, with further attenuation by co-silencing AKR1B1 and SORD. The effects of AKR1B1 and SORD knockdown were augmented under hyperglycemic conditions (Fig. 3A and Supplementary Fig. 3B). Cell numbers were not affected by the knockdowns (Supplementary Fig. 3C), indicating that the attenuation of cell migration does not result from cell injury. Moreover, hyperglycemia-induced cytoskeletal rearrangement and CDH1

suppression was attenuated by AKR1B1 and/or SORD knockdown (Fig. 3B, C and Supplementary Fig. 3D, E). An AKR1B1 enzyme inhibitor, epalrestat, also attenuated cell migration in AGS and MKN-45 (Supplementary Fig. 4A–D). When we ectopically expressed AKR1B1 in the AKR1B1-deficient gastric cancer cell lines SNU-601 and SNU-638 (Supplementary Fig. 2A), AKR1B1 increased cell migration and invasion under euglycemic conditions, which was augmented under hyperglycemic conditions (Fig. 3D and Supplementary Fig. 5A–D). In SORD-deficient MKN-1 cells, cell migration under hyperglycemic conditions was augmented by SORD overexpression (Fig. 3E and Supplementary Fig. 5E). Spearman correlation analysis using the GSE2685 gastric cancer database revealed that AKR1B1 expression was inversely correlated with CDH1 expression (Supplementary Fig. 5F). Collectively, our results suggest that the polyol pathway drives the hyperglycemia-induced migration and invasion of gastric cancer cells. Next, we tested the possibility that fructose is an effector of hyperglycemia-induced migration and invasion. As expected, fructose administration increased the intracellular levels of fructose (Fig. 3F, G), indicating that the cells can take up extracellular fructose through sugar transporters. Interestingly, intracellular fructose levels were also increased under hyperglycemic conditions, which was attenuated by silencing AKR1B1 in AGS and MKN-45 (Fig. 3F and Supplementary Fig. 6A, B). Overexpression of AKR1B1 increased the intracellular fructose levels in SNU-601 and SNU-638 (Fig. 3G and Supplementary Fig. 6A, C). In addition, L-fructose, which functionally competes with D-fructose, blocked the hyperglycemia-induced cell migration (Fig. 3H and Supplementary Fig. 6D and E) and CDH1 suppression (Fig. 3I and Supplementary Fig. 6F). These results suggest that hyperglycemia results in fructose generation through the polyol pathway, which in turn mediates EMT and cell migration.

High glucose triggers the fructose-dependent KHK-A signaling pathway

A recent study revealed the role of the ketohexokinase-A (KHK-A) signaling pathway in fructose-induced metastasis in breast cancer[27]. Exogenous fructose induces the nuclear translocation of KHK-A in association with KPNB1 and LRRC59 and in turn, KHK-A phosphorylates YWHAH, which recruits the repressor SLUG to the *CDH1* promoter. The CDH1 suppression induces EMT and subsequently triggers breast cancer metastasis (Fig. 4A). Based on this scenario, we hypothesized that endogenous fructose synthesized via the polyol pathway induces the KHK-A signaling pathway. KHK exists as two RNA splicing isoforms, KHK-A and KHK-C. KHK-C converts fructose to fructose-1-phosphate, whereas KHK-A regulates cell signaling as a protein kinase. In HepG2, AGS and MKN-45, KHK-A, rather than KHK-C, was predominantly expressed (Fig. 4B). Because ALDOB, ALOX12, and KHK-A have been reported to promote fructose-induced cancer metastasis[28, 29] (Supplementary Fig. 7A), we determined which of the three participated in hyperglycemia-induced cell migration. Cell migration was attenuated by KHK-A knockdown, but not by ALDOB or ALOX12 knockdown (Fig. 4C and Supplementary Fig. 7B, C, D). Immunofluorescence and immunoblotting analyses revealed that hyperglycemia induced the nuclear translocation of KHK-A alone (Fig. 4D, E and Supplementary Fig. 8A, B). We also found that KHK-A interacted with LRRC59 and KPNB1 under hyperglycemic conditions (Fig. 4F), and LRRC59 was found to

be essential for the hyperglycemia-induced nuclear translocation of KHK-A and cell migration (Fig. 4G, H, and Supplementary Fig. 8C).

The polyol pathway-derived fructose induces EMT through the KHK-A signaling pathway

Under high glucose and fructose conditions, KHK-A interacted with YWHAH (Fig. 5A) and phosphorylated YWHAH at S25 (Fig. 5B). More importantly, hyperglycemia-induced phosphorylation of YWHAH was almost completely attenuated by silencing AKR1B1 and/or SORD (Fig. 5C), strongly suggesting that polyol pathway-derived fructose drives S25-phosphorylation of YWHAH. Of the three *CDH1* repressors SNAIL, SLUG, and TWIST, YWHAH robustly interacted with SLUG in gastric cancer cells, which was inhibited by silencing AKR1B1 and/or SORD (Fig. 5D and Supplementary Fig. 9A). Given that the YWHAH_S25A mutant failed to interact with SLUG, the KHK-A-dependent S25-phosphorylation of YWHAH might be critical for the interactions under hyperglycemic conditions (Fig. 5E). Next, we observed that the polyol pathway was responsible for *CDH1* repression under hyperglycemic conditions (Fig. 5F and Supplementary Fig. 9B). Hyperglycemia-induced *CDH1* repression was rescued by YWHAH knockdown, and wild-type YWHAH, not the S25A mutant, repressed *CDH1* (Fig. 5G). The recruitment of SLUG to the *CDH1* promoter was augmented by hyperglycemia, which was attenuated by silencing AKR1B1 and/or SORD (Fig. 5H and Supplementary Fig. 9C). In contrast, SNAIL binding to the *CDH1* promoter was not regulated by the polyol pathway. We also found that S25-phosphorylation of YWHAH is critical for SLUG, not SNAIL, recruitment to the *CDH1* promoter in a glucose-dependent manner (Supplementary Fig. 10A). Moreover, S25-phosphorylation of YWHAH was critical for cell invasion under hyperglycemic conditions (Supplementary Fig. 10B). Taken together, these results suggest that polyol pathway-derived fructose enhances the metastatic potential of gastric cancer cells via the KHK-A-YWHAH-SLUG pathway.

Diabetes-induced metastasis of gastric cancer in a spleen-to-liver metastasis model

We next investigated whether the polyol pathway promotes gastric cancer metastasis in mice with diabetes. We used a model of spleen-to-liver metastasis because gastric cancer frequently metastasizes to the liver. We established stable cell lines of MKN-28, which are originally derived from intestinal gastric cancer, and verified AKR1B1 expression and luciferase activity (Supplementary Fig. 11A). The experimental schedule is shown in Fig. 6A. In streptozotocin (STZ)-treated mice of the groups ‘b’ and ‘d’, blood glucose levels were markedly increased to about 600 mg/dL (Fig. 6B). Significant weight loss was detected in group ‘d’ (Fig. 6C). By monitoring bioluminescence emission from cancer cells, we could observe more severe liver metastasis in diabetic controls than in non-diabetic controls. AKR1B1 overexpression promoted metastasis in non-diabetic mice and, to a greater extent, in diabetic mice (Fig. 6D, E). Histological examination of liver tissues verified that bioluminescence was emitted from metastasizing cancer cells (Fig. 6F). Representative images of liver metastases are shown in Supplementary Fig. 11B. We next examined whether diabetes-induced metastasis is driven by the KHK-A

signaling pathway. Nuclear localization of KHK-A/LRRC59 and S25-phosphorylation of YWHAH were significantly increased in AKR1B1-expressing tumors of diabetic mice (Fig. 6G and Supplementary Fig. 11C, D, E). In addition, CDH1 was downregulated in the liver metastases of diabetic mice, which was further augmented in AKR1B1-expressing tumors (Fig. 6H).

Diabetes-induced metastasis of gastric cancer in a subcutaneous xenograft model

For a subcutaneous xenograft model, SNU-638, which originally arose from a diffuse type of gastric cancer, was established to stably co-express luciferase and AKR1B1 (Supplementary Fig. 12A). Mice were randomly allocated to four groups (Fig. 7A). Blood glucose levels verified that diabetes was stably maintained after tumor implantation (Fig. 7B). In the diabetic group, the body weights of the mice declined in the late period of the experiment (Fig. 7C). On the 15th week after tumor injection, bioluminescence imaging analyses revealed tumor growth at the injection sites and abdominal metastases in AKR1B1-expressing tumors, which was further enhanced in diabetic mice (Fig. 7D). Values of region of interest (ROI) luminescence were used for the quantitative analysis of primary tumor growth and local tumor invasion (ROI 1) or distant metastasis (ROI 2 – ROI 1) (Fig. 7E). Bioluminescence emissions of the excised livers and intestines were robustly detected in group ‘d’ (Fig. 7F, G and Supplementary Figure. 12B), with weak emissions in groups ‘b and ‘c’, and little emission in group ‘a’. CA72-4 marked metastasizing cancer cells (Supplementary. Figure 13A, B). Moreover, nuclear localization of KHK-A/LRRC59, S25 phosphorylation of YWHAH, and suppression of CDH1 expression were significantly enhanced in group ‘d’ (Fig. 7H–J and Supplementary Fig. 13C–F). Collectively, these results suggest that diabetes promotes gastric cancer metastasis through the polyol and KHK-A signaling pathways.

Discussion

Most studies investigating the role of diabetes in cancer progression have focused on the signaling pathways and gene expressions altered by high glucose[16–18]. Here, we explored the mechanism by investigating the role of fructose rather than glucose *per se*. Under hyperglycemia, gastric cancer cells acquired an increased potential for migration and invasion with EMT, all of which occurred depending on fructose synthesis via the polyol pathway. Under hyperglycemia, the polyol pathway-derived fructose was sufficient to stimulate the KHK-A signaling pathway. In two different animal models mimicking gastric cancer metastasis, we found that metastasis was significantly increased in diabetic mice bearing AKR1B1-overexpressing tumors. Mechanistically, the polyol pathway-derived fructose triggered the nuclear translocation of KHK-A, which phosphorylated YWHAH and repressed the *CDH1* gene by recruiting SLUG to its promoter, thereby inducing EMT. Collectively, we propose that the connection between the polyol pathway and KHK-A signaling pathway plays a crucial role in diabetes-induced gastric cancer metastasis. Based on this mechanism, we also suggest that the enzymes AKRIB1 and KHK-A could be

potential targets for lowering metastatic risk in patients with gastric cancer. The polyol pathway and KHK-A signaling for gastric cancer metastasis are summarized in Fig. 8.

Gastric cancer is the fifth most common cancer and the third most common cause of cancer related deaths worldwide[2]. Several clinical studies have recently reported a significant correlation between diabetes and gastric cancer progression[11,13]. In addition, a meta-analysis revealed that hyperglycemia correlates with gastric cancer risk (HR, 1.11; 95% CI, 0.98–1.26)[30]. The 5-year survival rate of gastric cancer patients with diabetes is significantly lower than that of non-diabetic patients[31]. Although gastric cancer is highly prevalent, the clinical outcomes of patients without metastasis are favorable[32]. Indeed, gastrectomy is the best way to eradicate gastric cancers, and patients without the stomach can maintain relatively healthy lives with nutritional supplements. Thus, it is important to prevent metastasis in patients with gastric cancer. Our results provide a theoretical basis for strict control of hyperglycemia in cancer patients with diabetes to prevent metastasis.

According to Lauren's criteria, gastric cancer can be classified into intestinal and diffuse types[33]. The intestinal type forms localized masses removable surgically, but the diffuse type infiltrates into the surrounding tissues and shows a worse prognosis[33]. MKN-28 and SNU-638 were used as representative cells for intestinal and diffuse types, respectively. Considering such distinct properties of these cells, we also adopted two xenograft models: intra-splenic implantation of MKN-28 cells and subcutaneous implantation of SNU-638 cells. Interestingly, MKN-28 and SNU-638 metastasized to the liver in different histological patterns. Within mouse livers, MKN-28 formed large nodules, whereas SNU-638 infiltrated into the liver parenchyma without clumping. Even in tumor xenografts, gastric cancer cells may retain growth properties inherited from their origins.

Several studies have reported the effect of hyperglycemia on gene expression. Hyperglycemia induces MMP2 expression in cholangiocarcinoma by activating STAT3[34], upregulates MMP9 in lung cancer by inducing HMOX1[35], and upregulates MMP2/9 in breast cancer[36]. The upregulation of MMPs could be responsible for hyperglycemia-induced cancer metastasis[37]. In lung cancer cells, hyperglycemia induces TGF-β secretion, which stimulates EMT and cell migration[38]. Hyperglycemia also triggers the degradation of a p53 activator HIPK2[39], inhibiting he p53-dependent apoptosis[40]. HIF1A, which expresses many hypoxia-induced genes, is also upregulated by hyperglycemia and consequently induces VEGF and HMOX1, thereby promoting angiogenesis and tumor growth[41]. However, to the best of our knowledge, little is known about the signaling pathways that initiate these hyperglycemic effects. Moreover, it remains unclear how cancer cells sense glucose levels. Here, we suggest that polyol pathway-derived fructose stimulates cancer metastasis, and KHK-A appears to act as a fructose sensor.

ALDOB and ALOX12 have been reported to be involved in fructose-induced cancer metastasis[27–29]. KHK converts fructose to fructose-1-phosphate and ALDOB converts fructose-1-phosphate to glyceraldehyde and dihydroxyacetone phosphate. Colorectal cancer cells undergo metabolic reprogramming after liver metastasis. ALDOB is transcriptionally induced by GATA6 and promotes the fructose metabolism, which

provides metastasizing cancer cells with the energy and materials necessary for increased growth[28]. The lipoxygenase ALOX12 produces 12-HETE, which induces inflammation and promotes cancer progression[29, 42]. In breast cancer, fructose upregulates ALOX12 and a corresponding increase in 12-HETE, thereby promoting lung metastasis[29]. In contrast, KHK-A acts as a nuclear protein kinase upon fructose stimulation and represses *CDH1*, thereby facilitating breast cancer metastasis[27]. However, our results showed that fructose-induced cell migration and invasion were not attenuated by silencing either ALDOB or ALOX12, indicating that KHK-A primarily contributed to the pro-metastatic effect of fructose.

Several AKR1B1 inhibitors are in clinical trials as therapeutic drugs for diabetic complications[43, 44]. According to our results, AKR1B1 inhibitors could be potential drugs for preventing cancer metastasis in diabetic patients. If needed, AKR1B1 inhibitors can be co-administered with conventional anticancer drugs in cancer patients with diabetes. In some cases, AKR1B1 inhibitors could be used for dual purposes to inhibit diabetic complications or cancer exacerbation. On the other hand, KHK-A inhibitors could also have potential therapeutic benefits, and may prevent gastric cancer metastasis in diabetic patients. The KHK inhibitor PF-06835919, which is currently under clinical trials as a therapeutic agent for non-alcoholic steatosis and steatohepatitis[45], is an emerging agent for the prevention of cancer metastasis. Theoretically, it is plausible to try a combination therapy using AKR1B1 and KHK inhibitors to lower the risk of cancer metastasis in patients with diabetes.

Despite the high homology, KHK-A and KHK-C have different biochemical functions[46, 47]. Several studies have investigated the KHK-C-driven fructose flux as an underlying mechanism of fructose-induced cancer progression. High fructose levels have been reported to provide fuel and building blocks necessary for cancer growth and metastasis[28, 48]. However, it should be noted that KHK-A is predominantly expressed in most cancer cells, whereas KHK-C is rarely expressed. Since KHK-A has poor fructose phosphorylation activity, it is expected that fructose metabolism does not profoundly contribute to progression of most cancers lacking KHK-C. However, the endogenous role of KHK-A remains to be uncovered[27]. A recent study identified the function of KHK-A as a protein kinase. KHK-A enhances nucleic acid synthesis by phosphorylating and activating PRPS1, augmenting cell proliferation[49]. KHK-A also phosphorylates YWHAH, and consequently suppresses CDH1 expression, thereby promoting EMT and metastasis[27]. Based on these reports, KHK-A is likely to act as a protein kinase to facilitate cancer growth and metastasis.

Conclusion

We here report that the excessive production of fructose via the polyol pathway and the fructose-triggered KHK-A signaling pathway drives gastric cancer metastasis under hyperglycemic conditions. For patients with comorbidity of gastric cancer and diabetes, we strongly recommend strict control of blood glucose levels to prevent diabetes-induced cancer exacerbation. We also propose that the polyol and KHK-A signaling pathways could be potential targets to prevent and treat cancer metastasis in patients with diabetes.

Abbreviations

AKR1B1, aldo-keto reductase-1-member-1; EMT, epithelial-mesenchymal transition; KHK-A, ketohexokinase-A; SORD, sorbitol dehydrogenase; YWHAH, tyrosine 3-Monooxygenase/Tryptophan 5-Monooxygenase Activation Protein Eta; SLUG, snail family transcriptional repressor 2; KPNB1, karyopherin subunit beta 1; LRRC59, leucine rich repeat containing 59.

Declarations

Acknowledgements: We thank Su-Bin Kwak, Sang Jin Kim, and Chang Woo Ko for cooperative works and helpful discussion.

Author contributions: J.W.P. and Y.L.K. designed the study and wrote the manuscript. Y.L.K. and J.K. performed cell-based experiments and animal studies, and analyzed data and informatics. Y.S.K performed LC-MS. J.W.P. and Y.L.K. constructed expression vectors and established cell lines.

Funding: This study was supported by the National Research Foundation of Korea grant 2022R1A2C2091397 (J.W. P.).

Availability of data and materials:

Data, analytic methods, and study materials will not be made available to other researchers.

Ethics approval and consent to participate:

All animal experiments were performed in accordance with protocols approved by the Institutional Animal Care and Use Committee (approval No. SNU-190702-3-3).

Consent for publication: Not applicable.

Competing interests: All authors have no conflicts of interest.

References

1. Cho NH, Shaw J, Karuranga S, et al. IDF Diabetes Atlas: Global estimates of diabetes prevalence for 2017 and projections for 2045. Diabetes Res Clin Pract. 2018;138:271-281.
2. Sung H, Ferlay J, Siegel RL, et al. Global cancer statistics 2020: GLOBOCAN estimates of incidence and mortality worldwide for 36 cancers in 185 countries. CA: Cancer J Clin. 2021;71:209-249.
3. Yancik R, Ries LA. Aging and cancer in America: demographic and epidemiologic perspectives. Hematol Oncol Clin North Am. 2000;14:17-23.
4. Kirkman MS, Briscoe VJ, Clark N, et al. Diabetes in older adults. Diabetes Care. 2012;35:2650-2664.
5. Habib SL, Rojna M. Diabetes and risk of cancer. Int Sch Res Notices. 2013;2013:583786.

6. Chen H-F, Liu M-D, Chen P, et al. Risks of breast and endometrial cancer in women with diabetes: a population-based cohort study. PLoS One. 2013;8:e67420.
7. Giovannucci E, Harlan DM, Archer MC, et al. Diabetes and cancer: a consensus report. Diabetes Care. 2010;33:1674-1685.
8. Vigneri P, Frasca F, Sciacca L, et al. Diabetes and cancer. Endocr Relat Cancer. 2009;16:1103-1123.
9. Zhou X, Qiao Q, Zethelius B, et al. Diabetes, prediabetes and cancer mortality. Diabetologia. 2010;53:1867-1876.
10. Dankner R, Boffetta P, Balicer RD, et al. Time-dependent risk of cancer after a diabetes diagnosis in a cohort of 2.3 million adults. Am J Epidemiol. 2016;183:1098-1106.
11. Kim SK, Jang J-Y, Kim D-L, et al. Site-specific cancer risk in patients with type 2 diabetes: a nationwide population-based cohort study in Korea. Korean J Intern Med. 2018;35:641-651.
12. Chen Y, Wu F, Saito E, et al. Association between type 2 diabetes and risk of cancer mortality: a pooled analysis of over 771,000 individuals in the Asia Cohort Consortium. Diabetologia. 2017;60:1022-1032.
13. Shimoyama S. Diabetes mellitus carries a risk of gastric cancer: a meta-analysis. World J Gastroenterol. 2013;19:6902-6910.
14. Li W, Zhang L, Chen X, et al. Hyperglycemia promotes the epithelial-mesenchymal transition of pancreatic cancer via hydrogen peroxide. Oxid Med Cell Longev. 2016;2016:5190314.
15. Yu J, Hu D, Wang L, et al. Hyperglycemia induces gastric carcinoma proliferation and migration via the Pin1/BRD4 pathway. Cell Death Discov. 2022;8:1-10.
16. Li W, Zhang X, Sang H, et al. Effects of hyperglycemia on the progression of tumor diseases. J Exp Clin Cancer Res. 2019;38:1-7.
17. Duan W, Shen X, Lei J, et al. Hyperglycemia, a neglected factor during cancer progression. Biomed Res Int. 2014;2014:461917.
18. Ramteke P, Deb A, Shepal V, et al. Hyperglycemia associated metabolic and molecular alterations in cancer risk, progression, treatment, and mortality. Cancers. 2019;11:1402.
19. González RG, Barnett P, Aguayo J, et al. Direct measurement of polyol pathway activity in the ocular lens. Diabetes. 1984;33:196-199.
20. Yabe-Nishimura C. Aldose reductase in glucose toxicity: a potential target for the prevention of diabetic complications. Pharmacol Rev. 1998;50:21-34.
21. Chung SS, Ho EC, Lam KS, et al. Contribution of polyol pathway to diabetes-induced oxidative stress. J Am Soc Nephrol. 2003;14:S233-S236.
22. Schwab A, Siddiqui A, Vazakidou ME, et al. Polyol Pathway Links Glucose Metabolism to the Aggressiveness of Cancer Cells. Cancer Res. 2018;78:1604-1618.
23. Wu X, Li X, Fu Q, et al. AKR1B1 promotes basal-like breast cancer progression by a positive feedback loop that activates the EMT program. J Exp Med. 2017;214:1065-1079.

24. Saxena A, Shoeb M, Ramana KV, et al. Aldose reductase inhibition suppresses colon cancer cell viability by modulating microRNA-21 mediated programmed cell death 4 (PDCD4) expression. Eur. J Cancer. 2013;49:3311-3319.
25. Laffin B, Petrash JM. Expression of the aldo-ketoreductases AKR1B1 and AKR1B10 in human cancers. Front Pharmacol. 2012;3:104.
26. Li X, Yang J, Gu X, et al. The Expression and Clinical Significance of Aldo-Keto Reductase 1 Member B1 in Gastric Carcinoma. DNA Cell Biol. 2020;39:1322-1327.
27. Kim J, Kang J, Kang Y-L, et al. Ketohexokinase-A acts as a nuclear protein kinase that mediates fructose-induced metastasis in breast cancer. Nat Commun. 2020;11:1-20.
28. Bu P, Chen K-Y, Xiang K, et al. Aldolase B-mediated fructose metabolism drives metabolic reprogramming of colon cancer liver metastasis. Cell Metab. 2018;27:1249-1262.
29. Jiang Y, Pan Y, Rhea PR, et al. A sucrose-enriched diet promotes tumorigenesis in mammary gland in part through the 12-lipoxygenase pathway. Cancer Res. 2016;76:24-29.
30. Zheng J, Gao Y, Xie S-H, et al. Haemoglobin A1c and serum glucose levels and risk of gastric cancer: a systematic review and meta-analysis. Br J Cancer. 2022;126:1100-1107.
31. Tseng C-H. The relationship between diabetes mellitus and gastric cancer and the potential benefits of metformin: an extensive review of the literature. Biomolecules. 2021;11:1022.
32. Zhang Y, Lin Y, Duan J, et al. A population-based analysis of distant metastasis in stage IV gastric cancer. Med Sci Monit. 2020;26:e923867.
33. Ma J, Shen H, Kapesa L, et al. Lauren classification and individualized chemotherapy in gastric cancer. Oncol Lett. 2016;11:2959-2964.
34. Saengboonmee C, Seubwai W, Pairojkul C, et al. High glucose enhances progression of cholangiocarcinoma cells via STAT3 activation. Sci Rep. 2016;6:1-13.
35. Kang X, Kong F, Wu X, et al. High glucose promotes tumor invasion and increases metastasis-associated protein expression in human lung epithelial cells by upregulating heme oxygenase-1 via reactive oxygen species or the TGF-β1/PI3K/Akt signaling pathway. Cell Physiol Biochem. 2015;35:1008-1022.
36. Sun XF, Shao YB, Liu MG, et al. High-concentration glucose enhances invasion in invasive ductal breast carcinoma by promoting Glut1/MMP2/MMP9 axis expression. Oncol Lett. 2017;13:2989-2995.
37. Kapoor C, Vaidya S, Wadhwan V, et al. Seesaw of matrix metalloproteinases (MMPs). J Cancer Res Ther. 2016;12:28-35.
38. Alisson-Silva F, Freire-de-Lima L, Donadio JL, et al. Increase of O-glycosylated oncofetal fibronectin in high glucose-induced epithelial-mesenchymal transition of cultured human epithelial cells. PLoS One. 2013;8:e60471.
39. Baldari S, Garufi A, Granato M, et al. Hyperglycemia triggers HIPK2 protein degradation. Oncotarget. 2017;8:1190-1203.

40. Garufi A, D'Orazi G. High glucose dephosphorylates serine 46 and inhibits p53 apoptotic activity. J Exp Clin Cancer Res. 2014;33:1-10.
41. Wang Y, Zhu Y, Gui Q, et al. Glucagon-induced angiogenesis and tumor growth through the HIF-1-VEGF-dependent pathway in hyperglycemic nude mice. Genet Mol Res. 2014;13:7173-83.
42. Honn KV, Marnett LJ, Nigam S, et al. Eicosanoids and Other Bioactive Lipids in Cancer, Inflammation, and Radiation Injury 3. Springer Science & Business Media; 2013.
43. Ramirez MA, Borja NL. Epalrestat: an aldose reductase inhibitor for the treatment of diabetic neuropathy. Pharmacotherapy. 2008;28:646-655.
44. Schemmel KE, Padiyara RS, D'Souza JJ. Aldose reductase inhibitors in the treatment of diabetic peripheral neuropathy: a review. J Diabetes Complicat. 2010;24:354-360.
45. Futatsugi K, Smith AC, Tu M, et al. Discovery of PF-06835919: a potent inhibitor of ketohexokinase (KHK) for the treatment of metabolic disorders driven by the overconsumption of fructose. J Med Chem. 2020;63:13546-13560.
46. Basciano H, Federico L, Adeli K. Fructose, insulin resistance, and metabolic dyslipidemia. Nutr Metab. 2005;2:1-14.
47. Lanaspa MA, Andres-Hernando A, Orlicky DJ, et al. Ketohexokinase C blockade ameliorates fructose-induced metabolic dysfunction in fructose-sensitive mice. J Clin Invest. 2018;128:2226-2238.
48. Liu H, Huang D, McArthur DL, et al. Fructose Induces Transketolase Flux to Promote Pancreatic Cancer Growth. Cancer Res. 2010;70:6368-6376.
49. Li X, Qian X, Peng L-X, et al. A splicing switch from ketohexokinase-C to ketohexokinase-A drives hepatocellular carcinoma formation. Nat Cell Biol. 2016;18:561-571.

Figures

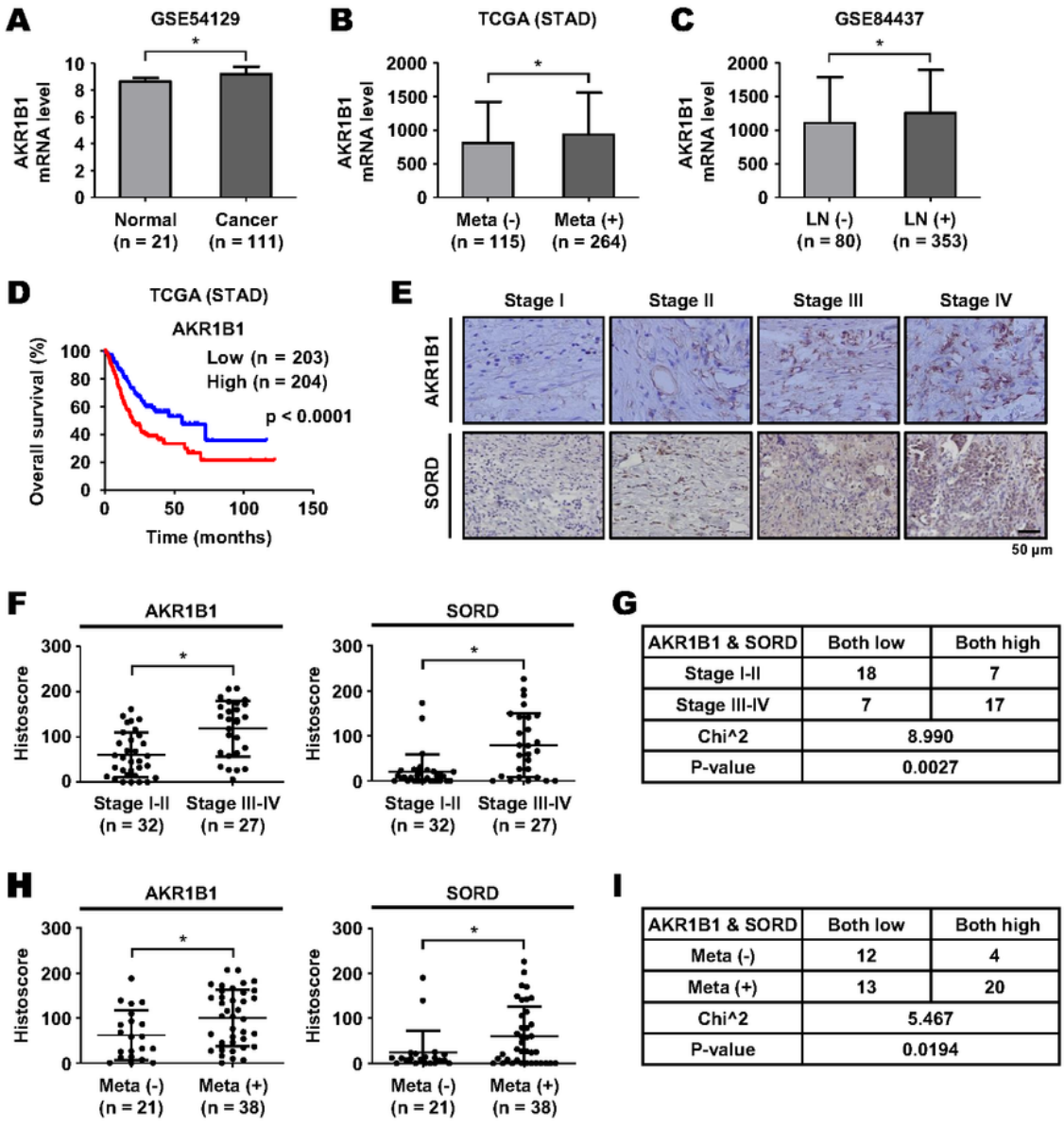

AKR1B1 & SORD	Both low	Both high
Stage I-II	18	7
Stage III-IV	7	17
Chi^2	8.990	
P-value	0.0027	

AKR1B1 & SORD	Both low	Both high
Meta (-)	12	4
Meta (+)	13	20
Chi^2	5.467	
P-value	0.0194	

Figure 1

The polyol pathway is clinically associated with gastric cancer metastasis.

A. AKR1B1 mRNA expression in normal stomach and cancer tissues. **B.** AKR1B1 mRNA expression in gastric cancer tissues of patients with and without metastasis. **C.** AKR1B1 mRNA levels in gastric cancer tissues of patients with and without lymph node metastasis. **D.** Kaplan–Meier analyses of the overall

survival in AKR1B1-low and -high gastric cancer patients. P value was calculated by log-rank test. **E.** Representative images of human gastric cancer tissues immuno-stained by anti-AKR1B1 or anti-SORD antibody. **F.** AKR1B1 and SORD protein levels in low-staged (I & II) and high-staged (III & IV) tumors. **G.** Chi-square analysis of AKR1B1/SORD expressions and tumor stages. **H.** AKR1B1 and SORD protein levels in non-metastatic and metastatic tumors. **I.** Chi-square analysis of AKR1B1/SORD expressions and metastasis. * denotes *P*< 0.05 by Mann-Whitney U test.

Figure 2

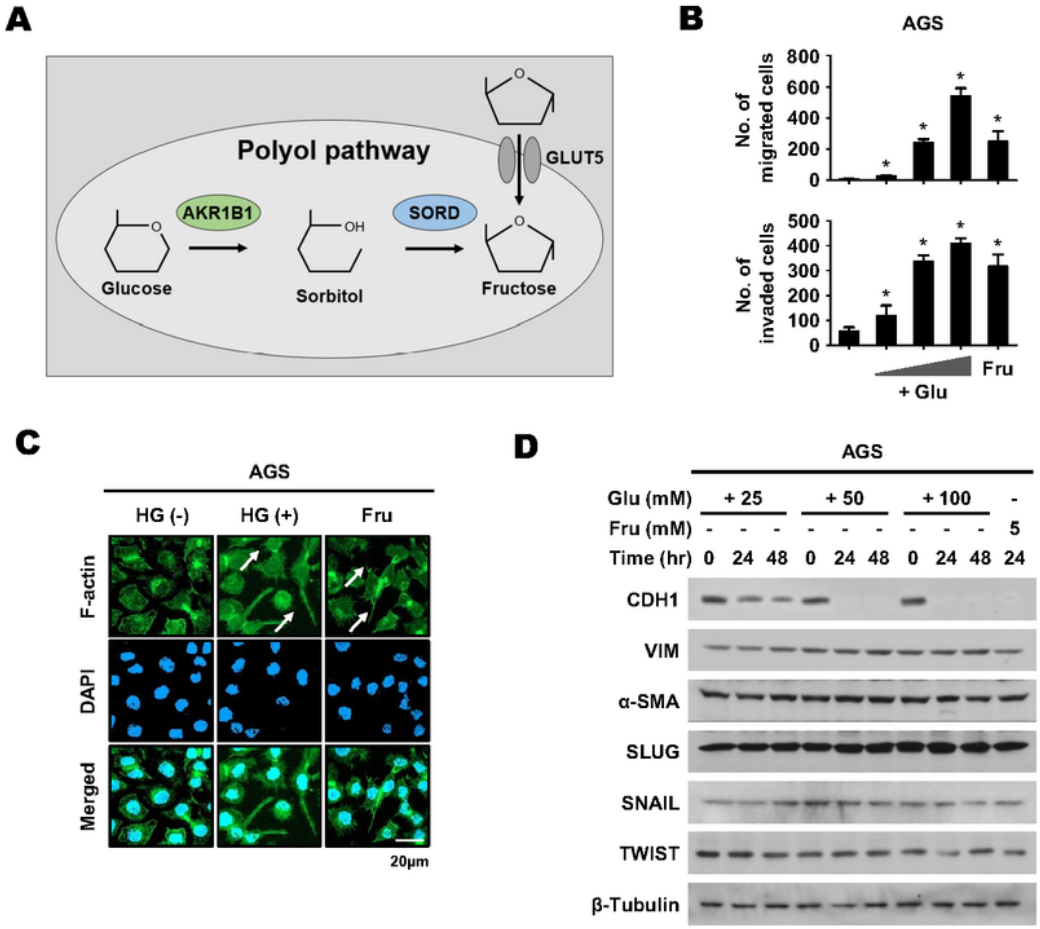

Figure 2

High glucose as well as fructose enhances metastatic potential in gastric cancer cells.

A. Graphical summary of polyol pathway. **B**. After 24 hr-incubation in the media supplemented with glucose (+ Glu; 25, 50, and 100 mM) or fructose (Fru, 5 mM), AGS cell migration and invasion were analyzed in Boyden chamber. The numbers of migrated or invaded cells are presented as bar graphs (means + SD, $n = 3$). * denotes $P < 0.05$ versus the euglycemic control. **C.** AGS cells were treated with high glucose (+ 50 mM glucose) or fructose (+ 5 mM) for 24 hr. F-actin (green) and nucleus (blue) were co-stained. White arrows indicate filopodia. **D.** AGS cells were treated with glucose or fructose for 24 or 48 hr, and subjected to Western blotting for EMT markers.

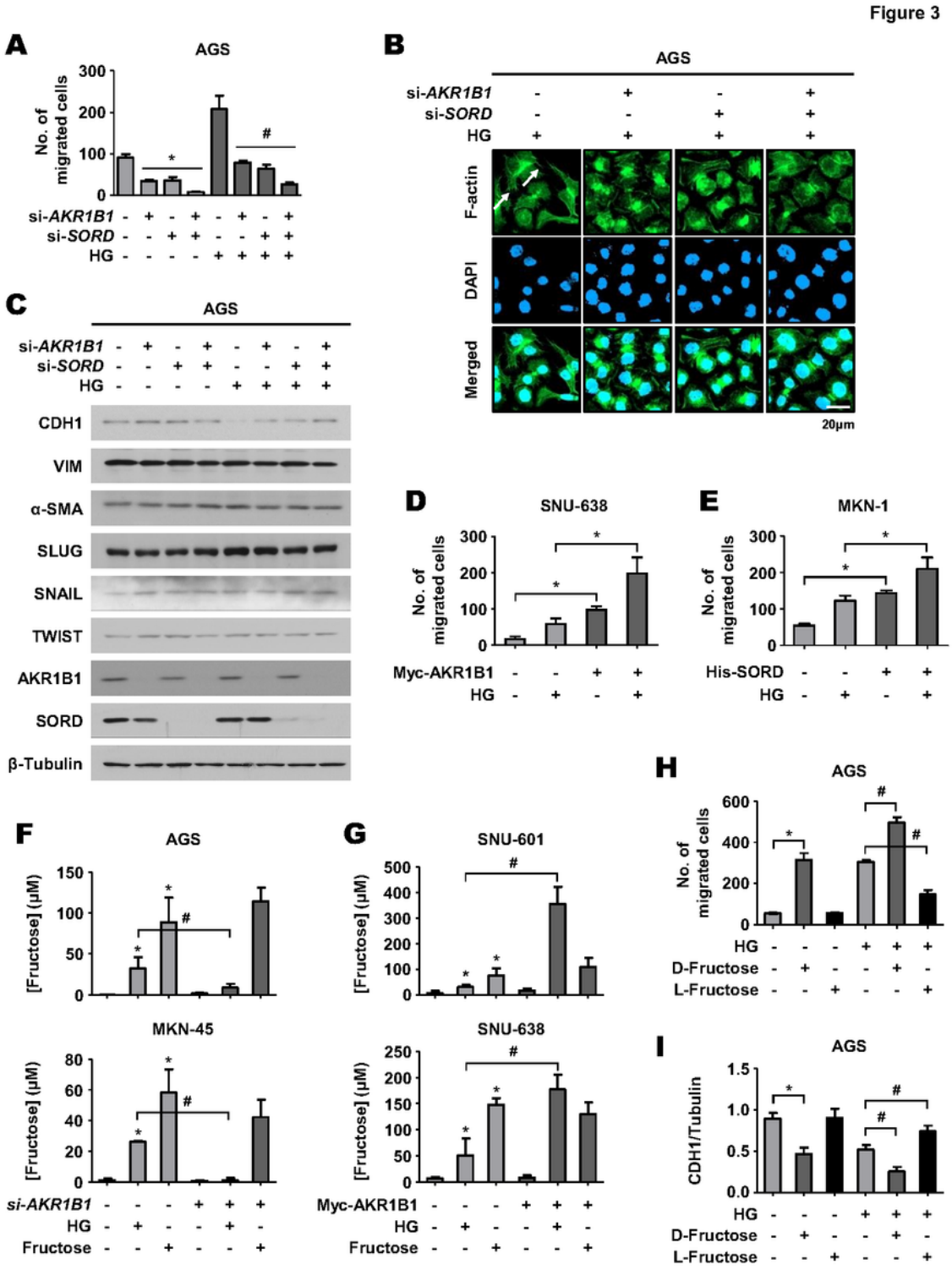

Figure 3

The polyol pathway augments the metastatic ability of gastric cancer under hyperglycemia.

A. AGS cells, which had been transfected with 80 nM si-RNAs, were treated with high glucose (HG) for 24 hr and subjected to migration assay. The numbers of migrated cells are presented as bar graphs (means + SD, $n = 3$). *, $P < 0.05$ versus the euglycemic control; #, $P < 0.05$ versus the hyperglycemic control. **B.** In

transfected cells treated as indicated for 24 hr, F-actin and nucleus were co-stained. White arrows indicate filopodia. **C.** AGS cells were transfected with si-RNAs, and incubated with high glucose for 24 hr. EMT protein markers were immunoblotted. **D.** SNU-638 cells, which had been transfected with Myc-AKR1B1, were treated with high glucose for 24 hr. Cells were subjected to migration assay (means + SD, $n = 3$). **E.** MKN-1 cells, which had been transfected with His(6)-SORD, were treated with high glucose for 24 hr, and subjected to migration assay. * denotes $P < 0.05$. (**F, G)**. AGS and MKN-45 cells were transfected with 80 nM si-AKR1B1. SNU-601 and SNU-638 cells were transfected with MYC-AKR1B1. After stabilized for 24 hr, cells were incubated with +50 mM glucose or +5 mM fructose for 24 hr. Cell extracts were subjected to MASS analyses to measure fructose levels. Fructose levels were normalized by packed cell volumes and presented as bar graphs (means + SDs, n = 3). **H.** AGS cells were treated with 5 mM D-Fructose, 5 mM L-fructose, and/or 50 mM glucose for 24 hr, and subjected to migration assay (means + SD, $n = 3$). **I.** AGS cells, which were treated as indicated, were subjected to immunoblotting for EMT markers. The blots of CDH1 and b-tubulin were quantified using ImageJ (means + SD, $n = 3$). * and # denote $P < 0.05$ versus the euglycemic control and the hyperglycemic control, respectively.

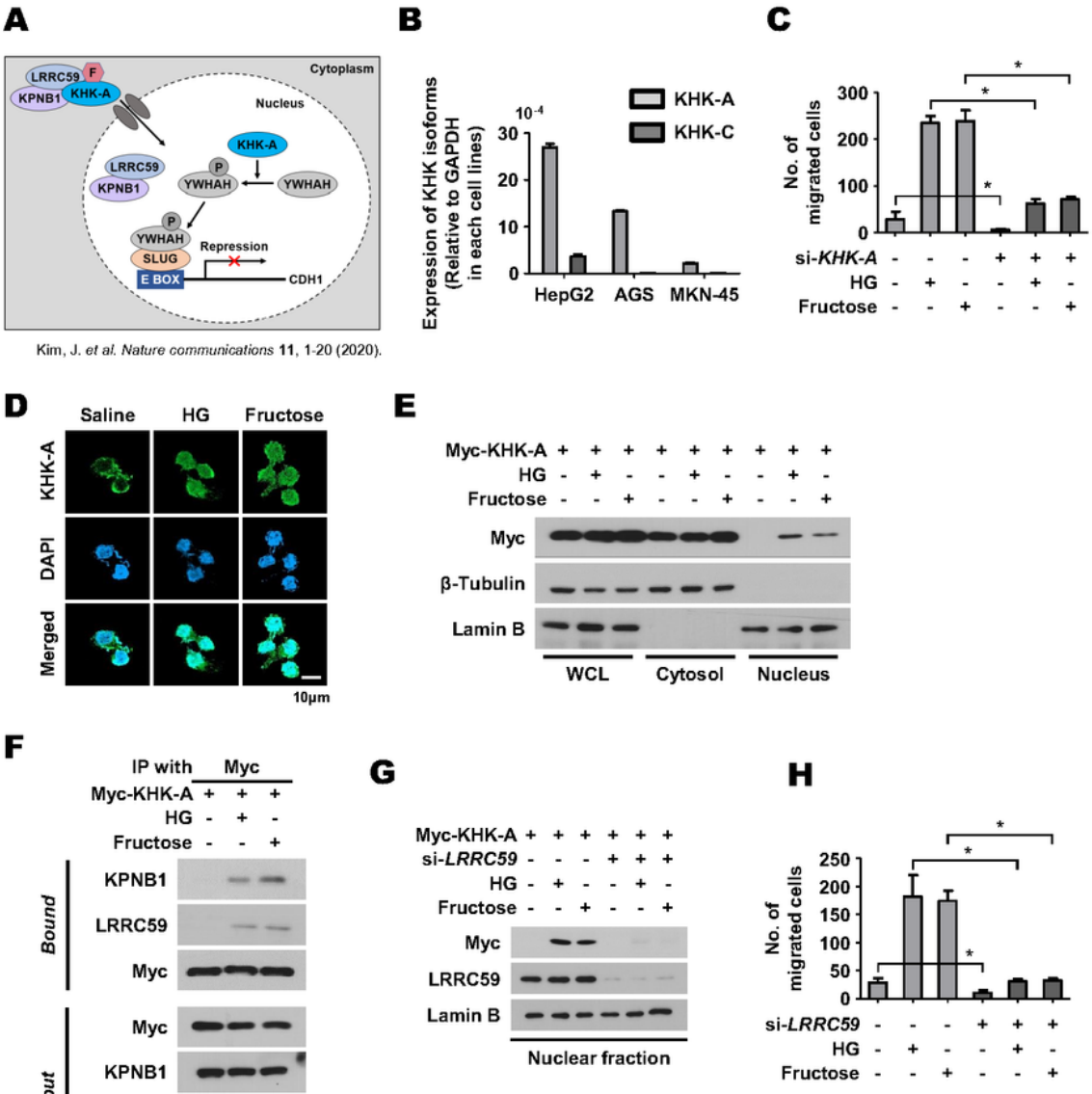

Figure 4

The polyol pathway-derived fructose activates the KHK-A signaling pathway.

A. The previously proposed mechanism for fructose-induced metastasis. **B.** The mRNA levels (means + SD, n = 3) of KHK-A and KHK-C were measured by quantitative RT-PCR. **C.** Transfected AGS cells were incubated with high glucose for 24 hr, and subjected to migration assay (means + SD, n = 3). * denotes *P*

< 0.05. **D.** AGS cells were incubated with high glucose or fructose for 24 hr, and immunostained (green KHK-A and blue DAPI). **E.** After transfected AGS cells were incubated with high glucose or fructose for 24 hr, cell lysates (WCL) were fractionated to the cytosolic and nuclear fractions and subjected to immunoblotting. **F.** Transfected AGS cells were treated with high glucose or fructose for 24 hr, and subjected to immunoprecipitation and immunoblotting. **G.** KHK-A was immunoblotted in the nuclear fraction from the transfected AGS cells incubated with high glucose or fructose for 24 hr. **H.** Transfected AGS cells were treated with high glucose or fructose for 24 hr, and subjected to migration assay (means + SD, $n = 3$). * denotes $P < 0.05$.

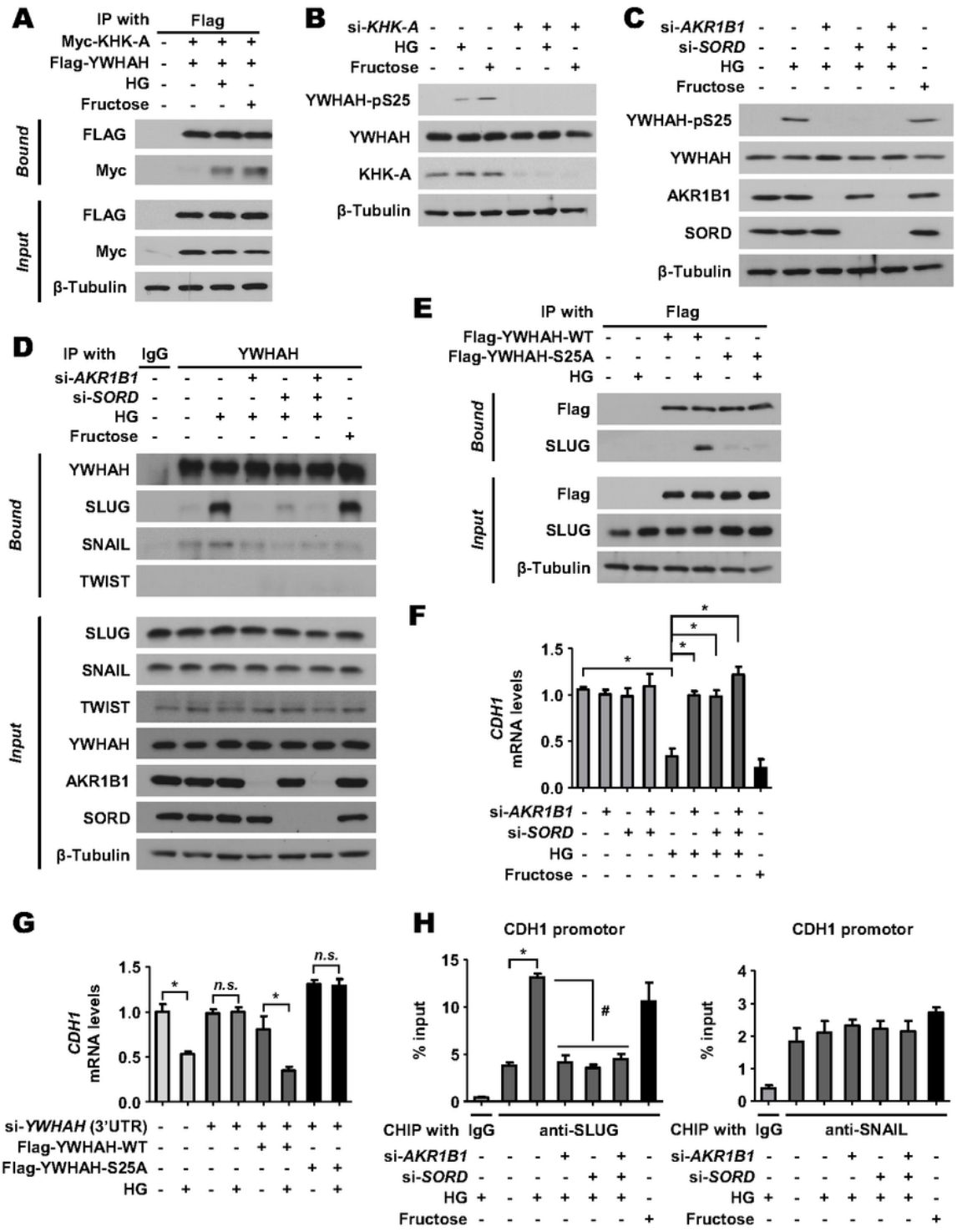

Figure 5

The polyol pathway-derived fructose induces EMT through the KHK-A signaling pathway.

A.AGS cells expressing Myc-KHK-A and Flag-YWHAH were incubated as indicted, and the cell lysates were immunoprecipitated and immunoblotted. **B.** In AGS cells, KHK-A-dependent phosphorylation of YWHAH at Ser25 was evaluated by immunoblotting. **C**. Transfected AGS cells were treated with high glucose or

fructose for 24 hr, and subjected to immunoblotting. **D.** AGS cells were subjected to immunoprecipitation and immunoblotting. **E**. The lysates of AGS cells expressing Flag-YWHAH (or S25A) were immunoprecipitated and immunoblotted. **F.** In AGS cells, The mRNA levels of CDH1 were analyzed by RT-qPCR (means + SD, n = 3). **G.** The mRNA levels (the mean + SD, n = 3) of CDH1 were measured by RT-qPCR in AGS. *, *P*< 0.05; *n.s.*, not significant. **H.** The transfected AGS cells were subjected to ChIP-qPCR using anti-SLUG or anti-SNAIL antibody. *, *P* < 0.05 versus the euglycemic si-control; #, *P*< 0.05 versus the hyperglycemic si-control.

Figure 6

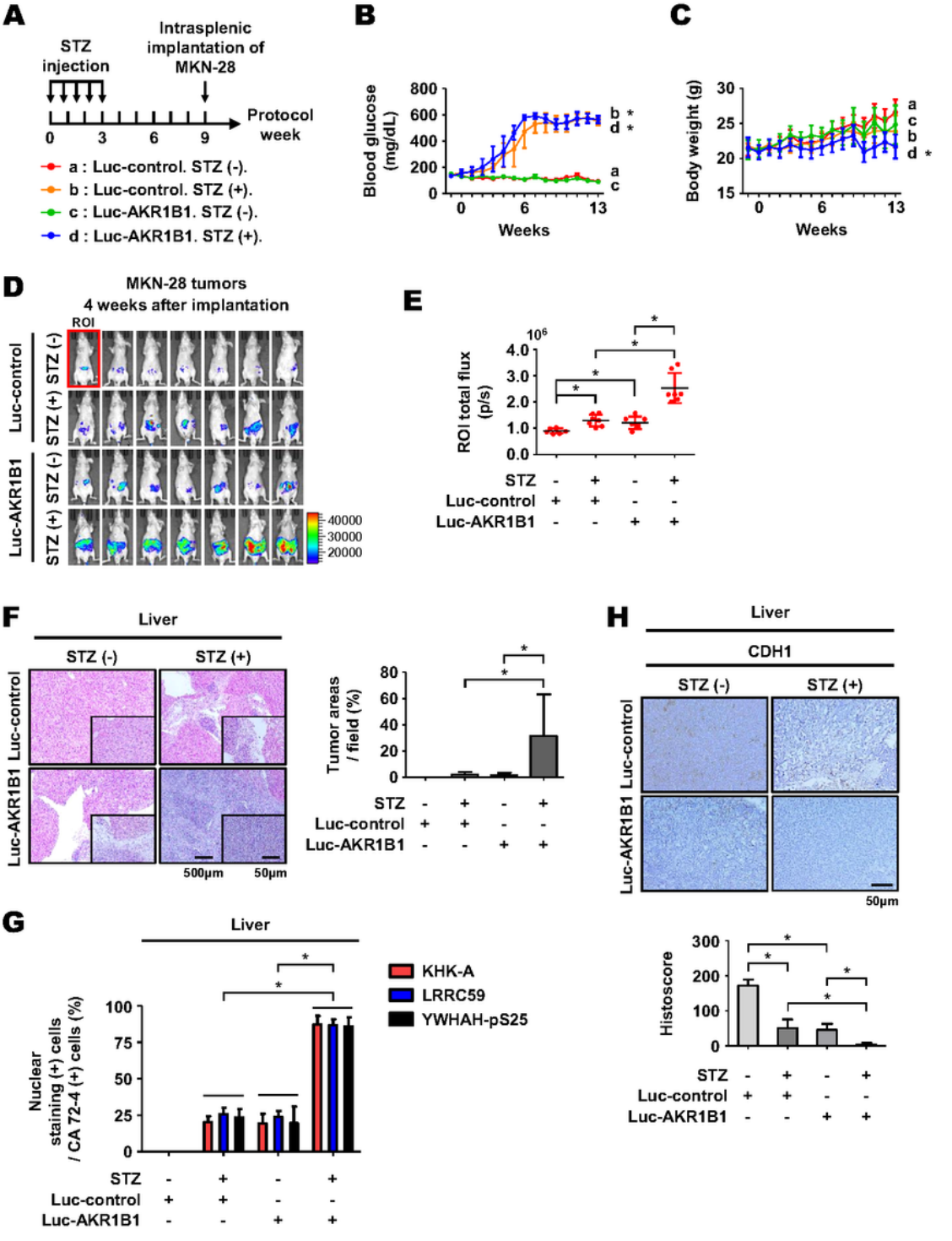

Figure 6

Hyperglycemia facilitates the spleen-to-liver metastasis of gastric cancer grafts in mice.

A. Schematic diagram of an animal model for hyperglycemia-induced metastasis of gastric cancer. Mice in the group b and d were intravenously injected with STZ. MKN-28 cells expressing luciferase and AKR1B1 (or GFP) were slowly implanted in the spleen using a syringe. Conditions for each experimental group (7 per each group) are described in the bottom panel. **B-C.** The blood glucose levels and body weights of mice were checked once a week. * denotes $P < 0.05$ versus the group 'a'. **D.** 4 weeks after the intrasplenic implantation of tumor cells, bioluminescence images of tumor-bearing mice were monitored using Xenogen IVIS spectrum. The color bar represents tumor intensity from purple (low) to red (high). **E.** Quantitative analysis of bioluminescence emission in total flux (photons/sec/cm^2/sr) measured 4 weeks after tumor implantation. **F.** On the 4^{th} week after tumor implantation, livers were excised from mice. Representative images of H&E-stained livers (left panel) and tumor areas per field were quantified using Image J (right panel). **G.** The excised livers were co-stained with the indicated antibodies and anti-CA72-4 antibody. All tissues were stained with fluorescent dyes to visualize. The percentage of nuclear KHK-A, LRRC59, or YWHAH-pS25 (+) cells in CA 72-4 (+) cells was counted and presented as bar graphs. **H.** Representative photographs of liver tissues immunostained with anti-CDH1 antibody (top panel). The expression levels were analyzed based on histoscore (bottom panel). Data in the graphs are presented as the means ± SD, and * denotes $P < 0.05$ (Mann-Whitney U test).

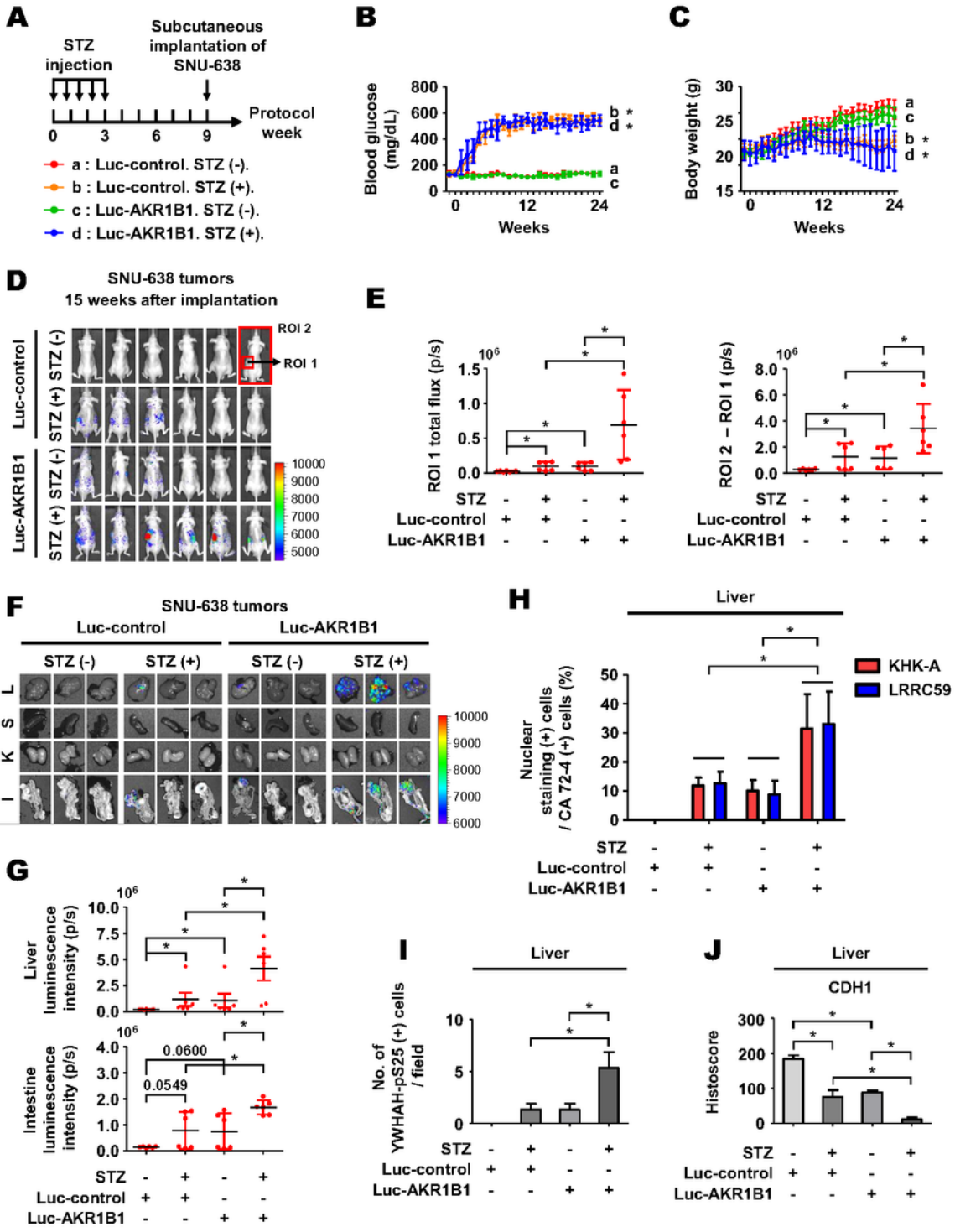

Figure 7

Hyperglycemia facilitates the distant metastasis of gastric cancer grafts in mice.

A. Schematic diagram of gastric cancer xenograft study. SNU-638 stable cells expressing luciferase and AKR1B1 (or GFP) were injected subcutaneously into the left flank of mice. Conditions for each experimental group (6 per each group) are described in the bottom panel.**B-C.** The blood glucose levels

and body weights of mice were checked once a week. *, $P < 0.05$ versus the group ‘a’. **D.** On the 15th week after tumor inoculation, the bioluminescence images of primary tumors and metastases were taken. **E.** Bioluminescence intensity of primary tumor (ROI 1) and metastases (ROI 2 – ROI 1) was quantitatively analyzed. **F.** Bioluminescence images in excised organs were captured (L = liver, S = spleen, K = kidney, I = intestine). Color bar represents tumor intensity from purple (low) to red (high). **G.** Quantitative analysis of bioluminescence emission in the livers and intestines. **H.** The excised livers were stained with the antibodies against KHK-A or LRRC59, and co-stained with anti-CA 72-4 antibody. To visualize protein expressions, fluorescent dyes were used. The percentage of nuclear KHK-A or LRRC59 expressions in CA72-4 (+) cells was quantified and presented as bar graphs. **I.** Livers were subjected to immunofluorescence staining. All tissues were stained with the antibody against YWHAH-pS25 and DAPI. **J.** The liver sections were immunostained with anti-CDH1, which were evaluated using histoscore. Data in the graphs are presented as the means ± SD, and * denotes $P < 0.05$ (Mann-Whitney U test).

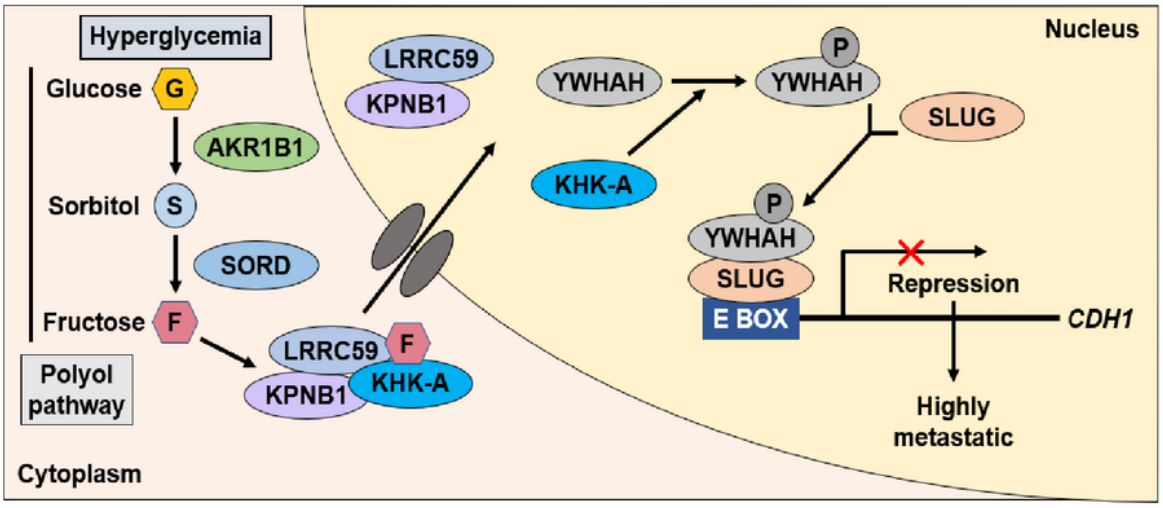

Figure 8

The proposed mechanism underlying diabetes-induced cancer metastasis.

In gastric cancer cells exposed to hyperglycemia, the polyol pathway produces excessive fructose, which stimulates the nuclear translocation of KHK-A. In the nucleus, KHK-A phosphorylates YWHAH and the

YWHAH in association with SLUG represses the *CDH1* gene. Consequently, gastric cancer cells undergo EMT due to the CDH1 repression, leading to metastasis under hyperglycemia.

Supplementary Files

This is a list of supplementary files associated with this preprint. Click to download.

- SupplementaryFiguresMolecularCancer.pdf
- SupplementaryTablesMolecularCancer.pdf